Journal of Experimental Botany, Vol. 58, No. 8, pp. 2033–2041, 2007
doi:10.1093/jxb/erm072 Advance Access publication 23 April, 2007
This paper is available online free of all access charges (see http://jxb.oxfordjournals.org/open_access.html for further details)

Journal of Experimental Botany
www.jxb.oxfordjournals.org

RESEARCH PAPER

Medicago truncatula ENOD40-1 and *ENOD40-2* are both involved in nodule initiation and bacteroid development

Xi Wan, Jan Hontelez, Allessandra Lillo, Chiara Guarnerio, Diederik van de Peut, Elena Fedorova, Ton Bisseling and Henk Franssen*

Laboratory of Molecular Biology, Department of Plant Sciences, Wageningen University, Dreijenlaan 3, 6703 HA, Wageningen, The Netherlands

Received 15 December 2006; Revised 12 March 2007; Accepted 13 March 2007

Abstract

The establishment of a nitrogen-fixing root nodule on legumes requires the induction of mitotic activity of cortical cells leading to the formation of the nodule primordium and the infection process by which the bacteria enter this primordium. Several genes are up-regulated during these processes, among them *ENOD40*. Here it is shown, by using gene-specific knock-down of the two *Medicago truncatula ENOD40* genes, that both genes are involved in nodule initiation. Further, during nodule development, both genes are essential for bacteroid development.

Key words: Bacteroid development, ENOD40, *Medicago truncatula*, nodule initiation, RNAi.

Introduction

Root nodules are specialized organs on the roots of legumes in which soil-borne bacteria, collectively known as rhizobia, are hosted intracellularly and fix atmospheric nitrogen. The formation of these organs requires a complex communication between the bacteria and their host plants. Plant-secreted flavonoids are inducers of bacterial genes that code for proteins involved in the production of so-called Nod factors. These molecules are lipo-chito-oligosaccharides consisting of a skeleton of 4,5 *N*-acetyl glucosamines, substituted with specific modifications (Spaink, 2000). Nod factors are recognized by plant receptors that activate a Nod factor signalling pathway. This induces mitotic activity in already differentiated cortical cells. These dividing cortical cells form the nodule primordium. Meanwhile, bacteria enter the root hair through a tube-like structure, the so-called infection thread. These threads grow towards the primordium and, upon arrival, bacteria are released from the threads. The bacteria become entrapped within the plant plasma membrane and form the so-called symbiosomes. After infection, the nodule primordium differentiates into a nodule (Stougaard, 2001; Limpens and Bisseling, 2003). *Medicago truncatula* nodules have a persistent meristem at their apex, and nodule cells are of graded age along the apical–basal axis. Therefore, based on both plant and rhizobial cell morphology (Vasse *et al*., 1990; Patriarca *et al*., 2004) and gene expression (Scheres *et al*., 1990), indeterminate nodules can be divided into four distinct zones, while five stages of bacterial development can be distinguished (Vasse *et al*., 1990; Patriarca *et al*., 2004). At the distal end, the meristem forms zone I. Cells of the meristem are small and rich in cytoplasm, while infection threads and bacteria are absent. Infection threads enter the cells at the distal end of zone II, the infection zone. Here, rhizobia are released from the infection threads and are surrounded by a plant membrane, together forming the symbiosome (rhizobia in stage I of development). The symbiosomes divide and the short rod-like rhizobia start to elongate (stage II). Rhizobia from this stage on are named bacteroids (Bergersen, 1974). In cells in the proximal part of the infection zone, bacteroids stop elongating and have a long rod-shaped structure (stage III). In cells of the fixation zone, zone III, the infected cells are fully packed with elongated bacteroids and the vacuoles of the cells have almost completely disappeared. At the distal part of the fixation zone, stage IV bacteroids are morphologically more heterogeneous and capable of fixing nitrogen. In older nodules, at the base of the nodule a zone can be distinguished where bacteroids disintegrate (stage V) and

* To whom correspondence should be addressed. E-mail: Henk.Franssen@wur.nl

plant cells begin senescence. This zone is called the senescence zone (zone IV).

During nodulation, several host genes are up-regulated, indicating that these genes are important for establishing a symbiosis between the plant and rhizobia. *ENOD40* is one of these genes (Kouchi and Hata, 1993; Yang *et al*., 1993; Crespi *et al*., 1994) and its expression level is increased at the onset of nodulation (Compaan *et al*., 2001). *ENOD40* is first expressed in pericycle cells and later in nodule primordium cells. Later in symbiosis *ENOD40* is expressed in cells of the nodule where differentiation of host cells and rhizobia is initiated.

ENOD40 has an unusual structure, since it lacks a long open reading frame (ORF). However, several short ORFs are present (Sousa *et al*., 2001) in *ENOD40* transcripts. Therefore, it is possible that these oligopeptides are translated and that a peptide represents the biological activity of *ENOD40*. Alternatively, due to the lack of a long ORF and the highly structured RNA (Girard *et al*., 2003), it has been suggested that the *ENOD40* activity resides in the RNA (Crespi *et al*., 1994; Sousa *et al*., 2001; Girard *et al*., 2003). At the nucleotide level, *ENOD40* transcripts share two regions of high sequence similarity, named box1 and box2 (Kouchi *et al*., 1999). Some of the short ORFs reside in these regions. In particular, a 10–13 amino acid oligopeptide encoded by the ORF in box1 is conserved among plant species (Compaan *et al*., 2001; Varkonyi-Gasic and White, 2002), with the exception of *Casuarina glutinosa* (Santi *et al*., 2003). The high degree of conservation of box1 and box2 sequences indicates that these regions are important for *ENOD40* function. However, it remains to be solved whether the *ENOD40* acitivity is peptide or RNA mediated.

The spatial and temporal expression of *ENOD40* suggests that this gene could play an important role in nodule development. Recently, it was reported that knock-down of *Lotus japonicus ENOD40* (*LjENOD40*) expression by RNA interference (RNAi) leads to a strong reduction in nodule number, but bacterial infection of root hairs was not affected (Kumagai *et al*., 2006). Also, in *M. truncatula*, *ENOD40* might be important in nodule initiation as in plants in which *ENOD40* expression is down-regulated due to co-suppression (Charon *et al*., 1999) nodule number is markedly reduced. Although these studies indicate that *ENOD40* has an important role in nodule initiation, none of the forward genetic screens for legume mutants disturbed in nodule formation has resulted in an *ENOD40* mutant. This might be due to functional redundancy or, alternatively, it indicates that *ENOD40* is not essential for nodule formation.

Several legumes, such as *Lotus* (Flemetakis *et al*., 2000) and *Trifolium repens* (Varkonyi-Gasic and White, 2002), have more than one copy of *ENOD40*. However, to date, only one *ENOD40* gene has been identified in *M. truncatula*. Recently, an expressed sequence tag (EST) has been deposited in the *M. truncatula* database, the nucleotide sequence of which shows homology to *Mt-ENOD40*. The identification of a putative second *MtENOD40* gene, *MtENOD40-2*, in *M. truncatula* opens up the possibility of testing whether both genes are required for nodule initiation and development.

To this end, gene-specific RNAi was applied to knock-down the expression of both genes separately in *M. truncatula* roots.

Materials and methods

Primers

The folowing primers were used: p402Hind, GGAAGCTTATCCTTAAGCTAAAAAAAAATCAGG; p402Bam, GGGGATCCATTTCAGTTATAGGATGATTC; Mt42Xba, GGTCTAGACAGGACCATTTGGAAAAATC; Mt42Bam, GGGGATCCAGAATCATACACACATACAG; Mt401SA, GGACTAGTGGCGCGCCGGTTTGCCATGCTAT; Mt401BS, GGGGATCCATTTAAATCCATCAAGACTTGAATCT; Mt402BS, GGGATCCATTTAAATGGATGAATCTTTGTTGGCAA; Mt402SA, GGACTAGTGGCGCGCCTAAGTGCAATGGTTGG; 401N1, GAGAAGTGTGAGAGGGTATTAAAC; 402N2, CAGTTACCTACCTTACTCATCTG; 402N1, GGATGAATCTTTGTTGGCAA; 402N2, ACTTGCCGGTTTACCAACCT; MtACTIN2F, TGGCATCACTCAGTACCTTTCAACAG; MtACTIN2R, CCCAAAGCATCAAATAATAAGTCAACC.

Plasmids and vectors

For the construction of the RNAi vector sil401, a DNA fragment containing 330 bp of the 5′-untranslated region (UTR) including box1 sequences was amplified using primers Mt401SA and Mt401BS, while for the construction of vector sil402 a DNA fragment comprising the 5′UTR including box1 of *MtENOD40-2* was amplified using primers Mt402BS and Mt402SA. Fragments were cloned into pGEM-T (Promega), yielding pGem401 and pGem402, respectively. Primers are provided with restriction enzyme recognition sites at their 5' end to facilitate subsequent cloning.

The amplified fragments were released from pGEM-T and cloned in two orientations by two sequential cloning steps in pBS-d35S-RNAi (Limpens *et al*., 2004), using *Asc*I and *Swa*I in the first cloning step and *Bam*HI and *Spe*I in the second step, respectively. The inverted repeat preceded by the 35S promoter was released by digestion and subsequently cloned in the binary vector pRedroot (Limpens *et al*., 2004) using *Kpn*I/*Pac*I restriction enzymes delivering the pRRsil401 and pRRsil402 vectors, respectively. To be able to knock-down the expression of *MtENOD40-1* and *MtENOD40-2* simultaneously, the *Spe*I–*Nco*I/blunted fragment of pGem401 and the *Bam*HI–*Ecl*I fragment of pGem402 were fused. The fragment obtained was then ligated into pGem402 from which the insert was removed after digestion with *Bam*HI and *Spe*I, yielding pGem4012. The insert of pGem4012 was then cloned in inverted orientation and used to generate pRRsil401 and pRRsil402; these were then introduced into pBS-d35S-RNAi. The inverted repeat obtained was then cloned into pBS-d35S-RNAi as described above and subsequently in pRedroot, yielding pRRsil4012.

To obtain the *MtENOD40-2* promoter sequence, a 1.8 kb DNA fragment upstream of the coding region of *MtENOD40-2* was obtained by PCR using primers p402Hind and p402Bam with BAC (bacterial artificial chromosome) DNA as template. The sequences of the primers were designed based on available nucleotide sequences of the 3.9 kb DNA fragment from the BAC clone that

hybridized to the *M. truncatula* EST BF519327. The obtained fragment was cloned into pCAMBIA1381Z digested with *Hin*dIII and *Bam*HI.

Plant transformation

Vectors were transformed with *Agrobacterium rhizogenes* MSU 440, containing the helper plasmid pRiA4 (Sonti *et al*., 1995), by means of electroporation.

Agrobacterium rhizogenes-mediated root transformation was performed according to Limpens *et al*. (2004). Nitrogen-starved plants were inoculated with *Sinorhizobium meliloti* SM2011. To prevent nitrogen deficiency, 15 d after inoculation with bacteria, plants were provided with Fahreus medium supplemented with 1.5 mM ammonium nitrate.

RNA isolation and reverse transcription mediated-PCR

At least five *M. truncatula* roots 2 weeks after transformation with *A. rhizogenes* were selected by screening for red fluorescence and collected for RNA isolation using the RNeasy Plant Mini Kit (Qiagen). As control, a similar number of roots that did not show red fluorescence were collected. Synthesis of cDNA and subsequent semi-quantitative reverse transcriptase-PCR was performed as described (Ruttink *et al*., 2006). Successful removal of genomic DNA was checked prior to cDNA synthesis. The rest of the plants were inoculated with *S. meliloti* SM2011 (Limpens *et al*., 2004).

Histochemical analyses, in situ *hybridization, and microscopy*

Histochemical analyses of β-glucuronidase (GUS) activity was performed as described by Limpens *et al*. (2005). Sections of 21-d-old nodules were generated as decribed (Limpens *et al*., 2005). [^{35}S]UTP-labelled RNA of *MtENOD40-2* was produced by T7 RNA polymerase on *MtENOD40-2* DNA cloned in plasmid pT7-5 (Scheres *et al*., 1990). Hybridization and subsequent detection and analyses of signal were performed as described (Limpens *et al*., 2005).

Sections of nodules for light and electron microscopy were obtained as described (Limpens *et al*., 2005).

Results

The Medicago truncatula *genome contains two* ENOD40 *genes*

The *M. truncatula* EST BF519327 has high homology to the 3′UTR of *MtENOD40* (GenBank Accession no. X80262). To obtain genomic sequences corresponding to the BF519327-encoding gene, a BAC library of *M. truncatula* (Nam *et al*., 1999) was screened with BF519327. A 3.9 kb DNA fragment from a BAC clone was sequenced, and this contained a new *ENOD40* gene, which has a region that is 100% identical to BF519327. Comparison of the nucleotide sequence of *MtENOD40-2* and *MtENOD40-1* (Fig. 1A) shows that the two genes only share 50% homology. Furthermore, the *MtENOD40-2* gene contains the two conserved boxes (Fig. 1A, B) present in all leguminous *ENOD40* genes identified to date, one of which contains an ORF for a small peptide (Fig. 1B). Whereas in all legumes the *ENOD40* peptide contains the motif C-W-(X3)-I-H-G-S, in the *MtENOD40-2* peptide the -I-H-G-S amino acid sequence is substituted by -I-Y-D (Fig. 1C).

On a Southern blot containing *Eco*RI-digested *M. truncatula* genomic DNA, the *MtENOD40-2* probe hybridized to two fragments, which is expected as *MtENOD40-2* contains one *Eco*RI site. In contrast, the *MtENOD40-1* probe hybridized to one fragment, as *MtENOD40-1* does not contain an *Eco*RI site (data not shown). Thus these data show that the *M. truncatula* genome contains two *ENOD40* genes.

MtENOD40-2 *is induced during nodulation*

To determine whether *MtENOD40-2* is expressed in nodule primordia and nodules, like *MtENOD40-1*, hairy roots containing a 1.8 kb DNA fragment upstream of the coding region of *MtENOD40-2* to drive the GUS reporter gene were analysed for GUS activity 2 d and 21 d after inoculation with *S. meliloti*. In sections of roots collected 2 d post-inoculation, GUS activity was present in dividing cortical cells, indicating that *MtENOD40-2* is expressed in cells of the nodule primordium (Fig. 2C). Whole-mount staining for GUS activity of nodules showed that GUS activity is detected near the apex of the nodule and in vascular bundles (Fig. 2D). To localize the site of expression of *MtENOD40-2* precisely in the nodule, *in situ* hybridization using [^{35}S]UTP-labelled antisense *MtENOD40-2* RNA was conducted (Fig. 2A, B). This showed that *MtENOD40-2* is expressed in cells of the infection zone (Fig. 2B, IZ). Thus, the *MtENOD40-2* expression pattern is similar to the *MtENOD40-1* expression pattern (Crespi *et al*., 1994). Furthermore, the *GUS* expression studies are consistent with the *in situ* hybridization data, indicating that the 1.8 kb DNA fragment used contains the elements required for the regulation of *MtENOD40-2* expression. Based on the combination of expression data and the sequence homology between both genes, it is likely that *MtENOD40-2* is functional in nodule initiation and development.

Gene specific knock-down of MtENOD40-1 *and* MtENOD40-2

To find out whether *MtENOD40-1* and *MtENOD40-2* are both required for nodule formation, the effect of reduction in expression of each gene individually on nodule formation has been investigated.

To reduce *MtENOD40-1* and *MtENOD40-2* gene expression, *A. rhizogenes*-mediated RNAi was applied in *M. truncatula* hairy roots (Limpens *et al*., 2004). To this end, one vector (pRRsil401) was designed that is expected to lead to a reduction in expression of *MtENOD40-1*, and a second vector (pRRsil402) that is expected to lead to a reduction in *MtENOD40-2* expression. To knock-down transcription of both genes simultaneously, a third vector (pRRsil4012) was used (Materials and methods).

Two-week-old transgenic roots were analysed for the levels of *MtENOD40-1* and *MtENOD40-2* transcripts by RT-PCR using *MtENOD40-1*- and *MtENOD40-2*-specific

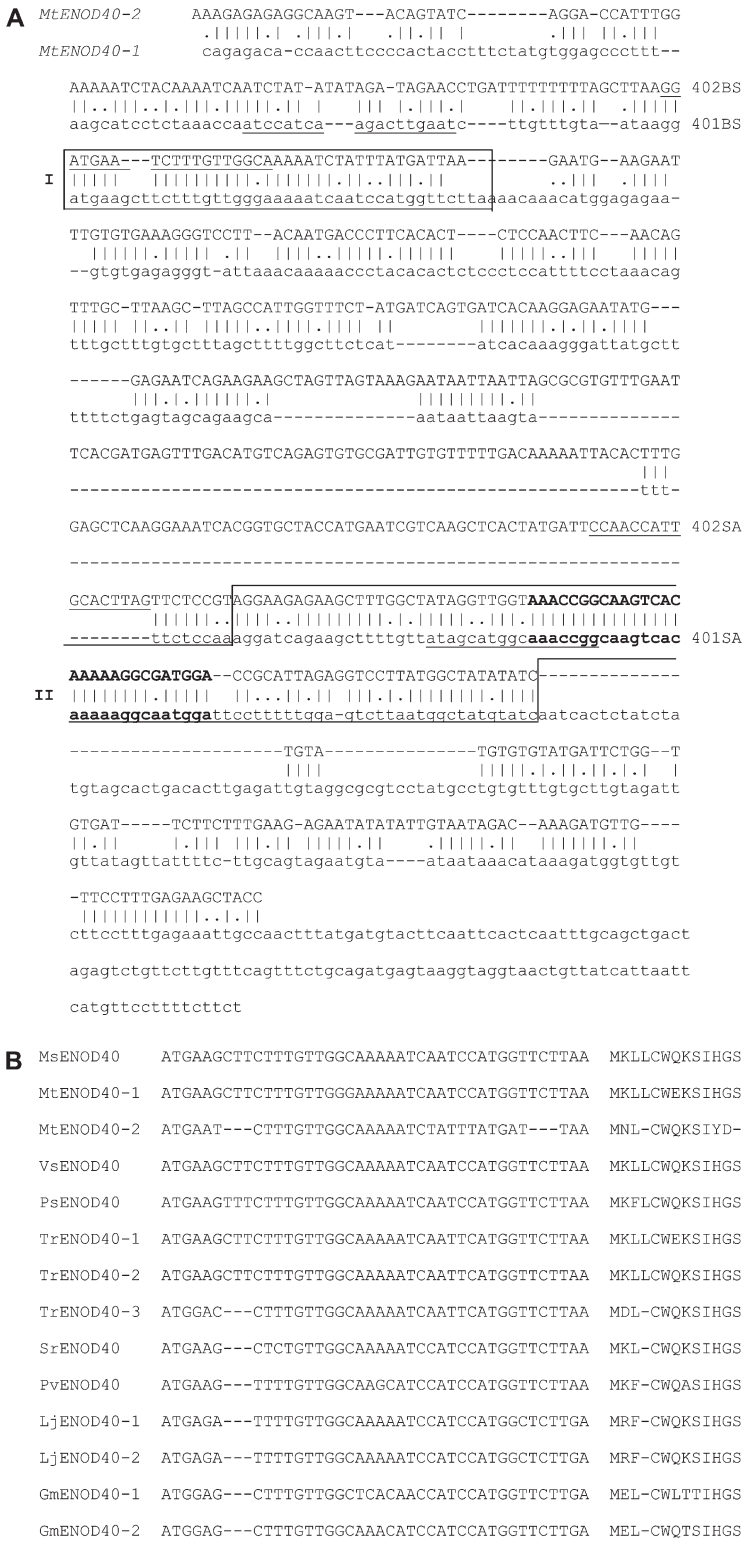

Fig. 1. Comparison of *MtENOD40* sequences. (A) Nucleotide sequence alignment of *MtENOD40-1* (lower case) and *MtENOD40-2* (upper case). Box1 and box2 sequences are boxed. Within box2, the nucleotide sequences conserved in all *ENOD40* sequences (Kouchi *et al*., 1999) are in bold. Nucleotide sequences of primers for gene-specific knock-down are underlined. Primer names are indicated on the right. (B) Nucleotide sequence alignment of box1 and amino acid sequence alignment of the ORF in box1 of legume *ENOD40* genes. Plant species abbreviations and GenBank accession nos: *MsENOD40*, *Medicago sativa* (L32806); *MtENOD40*, *Medicago truncatula* (1, X80264; 2, X80262); *VsENOD40*, *Vicia sativa* (X83683); *PsENOD40*, *Pisum sativum* (X81064); *TrENOD40*, *Trifolium repens* (1, AF426838; 2, AF426839; 3, AF426840); *SrENOD40*, *Sesbania rostrata* (Y12714); *PvENOD40*, *Phaseolus vulgaris* ((X86441); *LjENOD40*, *Lotus japonicus* (1, AF013594; 2, AJ271788); *GmENOD40*, *Glycine max* (1, X69154; 2, D13503).

primers (Fig. 3). The transcript level of *MtENOD40-1* was reduced about 25-fold in RNA isolated from *MtENOD40-1* RNAi roots as compared with that of control roots, that did not show red fluorescence (Fig. 3A, compare columns a and d), while *MtENOD40-2* expression was not altered in *MtENOD40-1* RNAi roots (Fig. 3B, compare columns a and d). In RNA isolated from *MtENOD40-2*-silenced roots, the transcript level of *MtENOD40-2* is reduced 5- to 25-fold compared with the transcript level in control roots (Fig. 3B, compare columns b and d), while the level of *MtENOD40-1* in *MtENOD40-2* RNAi and control roots is similar (Fig. 3B, compare columns a and d). Thus by using the pRRsil401 and pRRsil402, the expression of the two related genes *MtENOD40-1* and *MtENOD40-2* can be knocked down specifically. In roots containing RRsil4012 DNA, the level of the transcript of *MtENOD40-1* and *MtENOD40-2* is reduced >5-fold compared with the transcript levels of *MtENOD40-1* and *MtENOD40-2* in control roots (Fig. 3A, compare columns c and d; Fig. 3B, compare columns c and d). This shows that application of pRRsil4012 leads to a reduction in expression of both *MtENOD40-1* and *MtENOD40-2*.

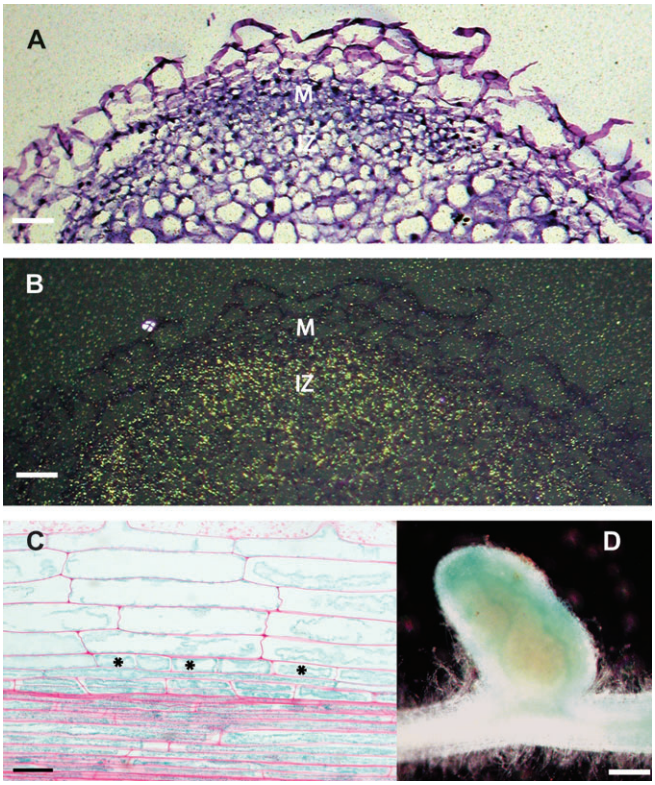

Fig. 2. Expression of *MtENOD40-2* during nodulation. (A, B) *In situ* hybridization of a longitudinal section hybridized to [^{35}S]UTP-labelled antisense *MtENOD40-2* RNA. Bright field micrograph (A). Dark field micrograph (B), where the signal appears as white grains. Signal is present in the infection zone (IZ) and absent from the meristem (M). Bar=200 μm. (C) Histochemical localization of GUS activity in a semi-thin (7 μM) section of *pMtENOD40-2:GUS* roots, 2 d after inoculation with *S. meliloti*. Dividing cortical cells are indicated by an asterisk (*). Bar=25 μm. (D) Whole-mount detection of *pMtENOD40-2:GUS* activity in 21-d-old nodules, showing promoter activity in the apical part of the nodule and in vascular bundles. Bar=0.5 mm.

Reduced nodule number in MtENOD40-1 *and* MtENOD40-2 *knock-downs*

Nodules formed on roots in which the *MtENOD40-1* and *MtENOD40-2* genes are knocked down were determined 3 weeks after inoculation (Table 1).

Whereas an average of 3.2 nodules/*MtENOD40-1* RNAi root was formed, 5.9 nodules/root are formed on control roots (46.4% reduction). On *MtENOD40-2* RNAi roots, the average number of nodules per root was 3.4, which corresponds to a reduction in nodule numbers of 38.5%. These data indicate that *MtENOD40-1* as well as *MtENOD40-2* is involved in nodule initiation. On roots, in which the expression of both *MtENOD40-1* and *MtENOD40-2* is reduced, the average number of nodules per root is 1.5 (75% reduction). Thus knocking down of the expression of both genes has an additive effect, suggesting that *MtENOD40* acts in a dose-dependent manner.

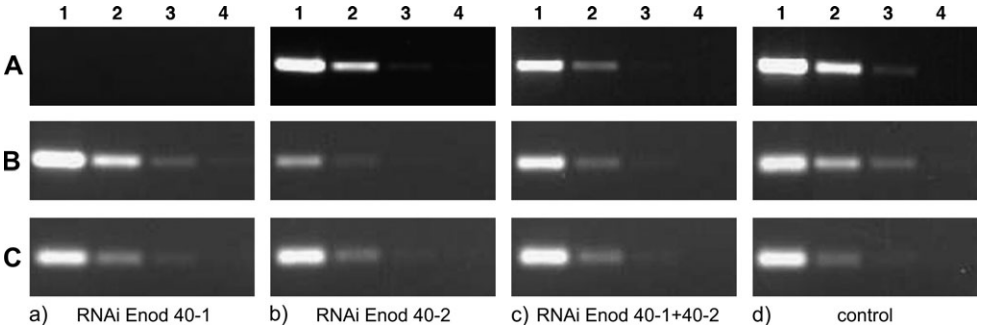

Fig. 3. RT-PCR analyses of *MtENOD40-1* and *MtENOD40-2* expression in knock-down roots using gene-specific primers. (A) *MtENOD40-1* RNA level in *MtENOD40-1* RNAi (column a), *MtENOD40-2* RNAi (column b), and double RNAi (column c). Reduction of *MtENOD40-1* RNA level in *MtENOD40-1* RNAi and double RNAi, but not in *MtENOD40-2* RNAi (column b) roots, compared with control roots (column d). (B) *MtENOD40-2* RNA level in *MtENOD40-1* RNAi (column a), *MtENOD40-2* RNAi (column b), and the double RNAi (column c). The *MtENOD40-2* RNA level is reduced in *MtENOD40-2* RNAi and double RNAi, but not in *MtENOD40-1* RNAi roots, compared with control roots (column d). (C) *Mtactin2* RNA levels. Amplification is shown in 0- (1), 5- (2), 25- (3), and 125-fold dilutions (4) of the cDNA mix at a fixed number of cycles; 30 cycles for *MtENOD40-1*, 30 cycles for *MtENOD40-2*, and 22 cycles for *Mtactin*.

Reduced MtENOD40-1/40-2 *expression affects symbiosome development*

To determine whether *MtENOD40-1* and *MtENOD40-2* are required for nodule development, nodules formed on *MtENOD40-1* and *MtENOD40-2* RNAi plants were analysed in more detail. Whereas 3-week-old nodules on control plants are rod shaped (Fig. 4A), the nodules formed on *MtENOD40-1* or *MtENOD40-2* RNAi plants are spherical and small (Fig. 4E). Longitudinal sections were prepared from control nodules and nodules of *MtENOD40-1* or *MtENOD40-2* RNAi roots to analyse their cytology.

Table 1. *Effect of RNAi on number of nodules*

	Nodules/root	Reduction
MtENOD40-1 RNAi	3.2±0.3 (*n*=51)	46.4% (*P* <0.001)
Wild type	5.9±0.2 (*n*=61)	
MtENOD40-2 RNAi	3.4±0.2 (*n*=55)	38.5% (P <0.01)
Wild type	5.5±0.2 (*n*=62)	
MtENOD40-1 and *-2* RNAi	1.5±0.2 (*n*=60)	75.0% (*P* <0.000001)
Wild type	6.0±0.3 (*n*=62)	

Analyses of sections of *MtENOD40-1* RNAi nodules showed that in about half of the *MtENOD40-1* RNAi nodules (Fig. 4F, J), the zonation of the central tissue cannot be recognized (compare Fig. 4A–D and 4F, J). The majority of these nodules were senescent. Some cells in the proximal part are repopulated by rhizobia. These are

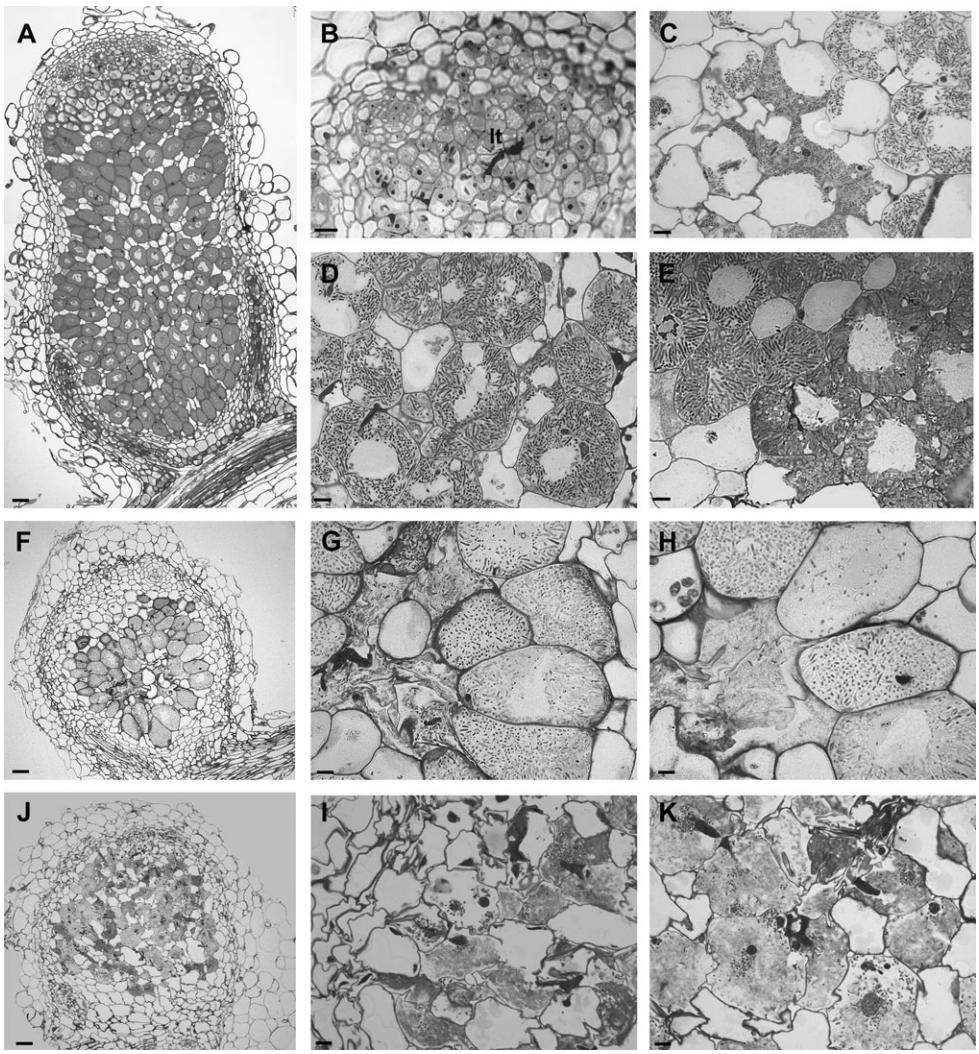

Fig. 4. Histology of 3-week-old RNAi nodules (F–K) compared with control nodules (A–E). Light microscopy of a control nodule (A–E). (A) Median longitudinal section of a 3-week-old nodule. (B) Magnification of the meristem and the distal part of the infection zone of a wild-type nodule, where bacteria are released from infection threads (It). (C) Magnification of the infection zone, where short rod-shaped bacteriods are present at the distal part, and (D) long rod-shaped bacteroids in the proximal part. (E) Magnification of the fixation zone containing cells fully packed with elongated bacteroids. (F) Light microscopic analyses of a longitudinal section of an aberrant *MtENOD40-1* RNAi nodule. Note that the zonation is not clear. (G) A senescent nodule wherein cells in the middle of zone III lost turgor and collapsed. (H) Note the size of bacteroids compared with bacteroids in (E). (J) A dead nodule recolonized by saprophytic rhizobia. (I) Magnification of collapsed cells being repopulated with bacteria. (K) Release of rhizobia from intracellular colonies. Bars=20 μm.

rod shaped, and electron microscopy (EM) studies show that they lack a plant-derived membrane and the ultrastructural differentiation features of bacteroids. Therefore, the bacteria colonize cells in a saprophytic manner (Timmers *et al*., 2000; Fig. 4J, K). In about half of the *MtENOD40-2* RNAi and 40% of the nodules from plants in which the expression of both genes was reduced, growth disturbances are similar to those observed in the *MtENOD40-1* RNAi nodules.

Among the nodules studied, nodules that were less disturbed in their development were also identified (Fig. 4F–H). In cells of the infection zone of these nodules, a few bacteria are released from the infection threads and can be recognized as small rod-shaped bacteroids. However, bacteroids remain short and rod shaped. At later stages of development, in the middle of the nodule lysed cells with an irregular shape that lost turgor are present (Fig. 4F, G) as well as senescent cells (Fig. 4G, H). Thus light microscopy (LM) analyses showed that bacteroid development was impaired. To identify which step in bacteroid development is affected, bacteroids in these nodules were studied by EM.

In *MtENOD40-1* RNAi nodules (Fig. 5A, B), bacteria are released from infection threads, and EM analyses revealed that each bacteroid was surrounded by symbiosome membrane as in the wild type (Fig. 5C). In contrast to wild-type nodules, bacteroid development was arrested at stage II–III and never developed into bacteroids of stage IV (Fig. 5). Further, in cells of the fixation zone, bacteroids undergo premature senescence (Fig. 5D). This is characterized by the presence of electron-dense cytoplasm, an enlarged peribacteroid space, and an irregular shape. Furthermore, in cells of this zone, fusion of symbiosomes leads to the formation of vacuole-like structures with lysis of bacteroids that are trapped inside (Fig. 5E). The latter is a typical feature for (premature) symbiosis termination (Vance and Johnson, 1983; Vasse *et al*., 1990). The bacteroid lysis was followed by destruction of mitochondria, as cells contained swollen organelles with degraded matrix and a very low number of cristae (Fig. 5E). These observations show that senescence of both partners occurs concomitantly. Analyses of *MtENOD40-2* RNAi and nodules in which the expression of both *MtENOD40* genes is reduced also showed that bacteroid development was blocked at stage II–III. These data indicate that reduction of the *MtENOD40-1* and *MtENOD40-2* expression levels in nodules interfered with bacteroid development. Strikingly, irrespective of which gene is knocked down, the percentage of the nodules with growth disturbances is similar (~50%). This indicates that *MtENOD40-1* and *MtENOD40-2* genes are not acting redundantly.

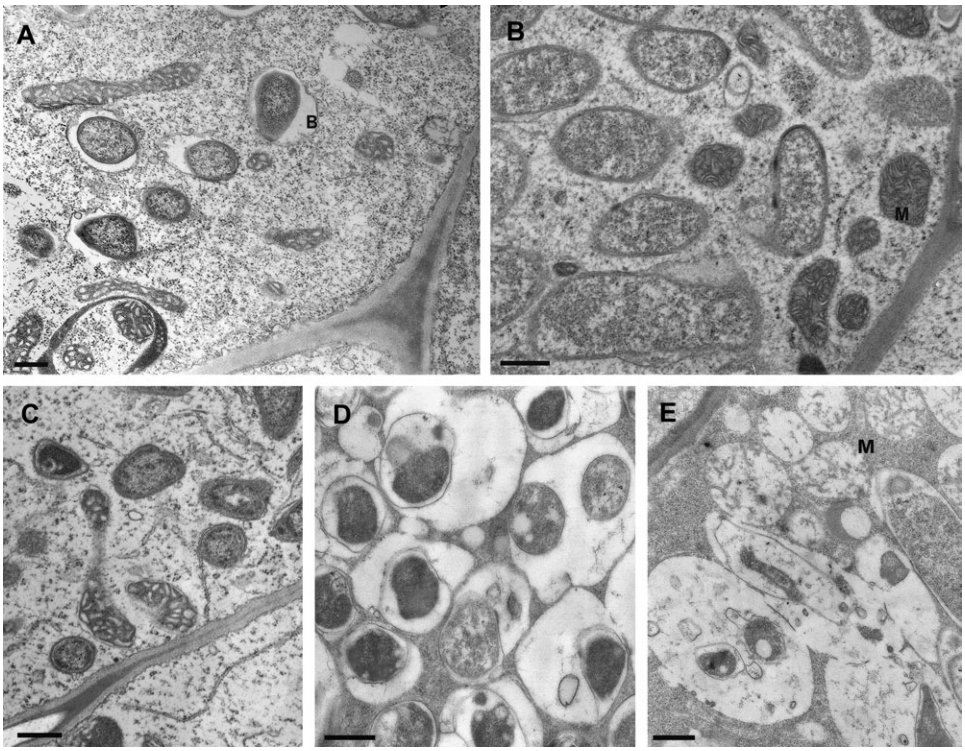

Fig. 5. Ultrastructure of control (A and B) and 3-week-old RNAi nodules (C, D, and E). (A) Wild-type nodules; young bacteroids in the distal part of the infection zone. (B) Wild-type nodules; proximal part of the infection zone. (C) RNAi nodules; infection zone. (D) Bacteroids with a large peribacteroid space, fusing. (E) Lysis of bacteroids entrapped inside a vacuole-like structure. Note swollen mitochondria of the host cell (B, bacteroids; M, mitochondria. Bars= 500 nm).

Discussion

Here the identification of a second *MtENOD40* gene, *MtENOD40-2*, and the involvement of this gene in nodule formation were described.

MtENOD40-2 contains the two regions, box1 and box2, that are conserved among all *ENOD40* genes known so far. However, whereas all legume *ENOD40* genes contain an ORF encoding a peptide with the conserved amino acid motif -C-W-(X3)-I-H-G-S, the peptide encoded within the ORF of *MtENOD40-2* lacks the three C-terminal amino acids -H-G-S. It is not clear whether the activity of *ENOD40* is determined by the peptide encoded within box1 of *ENOD40*. Hence, the significance of the change in amino acid order of *MtENOD40-2* peptide with respect to activity of *MtENOD40-2* remains unknown.

ENOD40 gene expression has been shown to be highly induced during the interaction of the roots of legumes with *Rhizobium*. Here, it is shown that *MtENOD40-2* is expressed in the nodule primordium and in the infection zone of the nodule, like *MtENOD40-1*. Co-localization of different *ENOD40* genes within one species has also been shown in *Medicago sativa* (Fang and Hirsch, 1998), *L. japonicus* (Flemetakis *et al*., 2000), and *T. repens* (Varkonyi-Gasic and White, 2002). Although the levels of *MtENOD40-1* and *MtENOD40-2* expression in nodules have not been compared, the detection of 42 ESTs for *MtENOD40-1* among several cDNA libraries of *M. truncatula* nodules (http://www.tigr.org/tigr-scripts/tgi/T_index.cgi?species=medicago;http://medicago.toulouse.inra.fr/Mt/EST/), compared with one for *MtENOD40-2*, strongly indicates that *MtENOD40-1* is much more highly expressed in nodules than *MtENOD40-2*.

The spatial and temporal expression pattern of *MtENOD40-1* and *MtENOD40-2* during nodule formation suggests a role for these genes in this process. In *M. truncatula*, knock-down of *MtENOD40-1* expression led to a 50% reduction in the number of nodules (Charon *et al*., 1999), and RNAi of *LjENOD40-1* in *L. japonicus* led to an even more drastic reduction in nodule numbers. Thus, these data all show that *ENOD40* is involved in nodule initiation. However, since in both experiments the introduced *ENOD40-1* DNA contained the conserved box2 sequences, the observed reduction in nodule number cannot be assigned to the reduction of *ENOD40-1*, *per se*. Here it is shown, by using a gene-specific knock-down, that *MtENOD40-1* and *MtENOD40-2* are both involved in nodule initiation. The observation that a decrease in expression levels of either *MtENOD40-1* or *MtENOD40-2* reduces nodule initiation suggests that the two *MtENOD40* genes do not act redundantly in nodule initiation. Further, as a reduction of the expression of both *MtENOD40* genes leads to a higher reduction of nodule initiation, the effect on nodule initiation of the *MtENOD40* genes is synergistic. Therefore, it is proposed that the effect of *MtENOD40* on nodule initiation is dose dependent. This dose-dependent effect of *ENOD40* genes on nodule initiation explains why no mutant in *ENOD40* came out of the genetic screens for mutants impaired in nodule initiation. In both *L. japonicus* and *M. truncatula*, a reduction, but not a complete knock-down, in *ENOD40* expression leads to significant inhibition of nodule formation. Therefore, the present results and the results in *L. japonicus* (Kumagai *et al*., 2006) strongly suggest that *ENOD40* genes are essential for nodule initiation.

Furthermore, it is shown that in all knock-downs tested, the percentage (50%) of aberrant nodules formed is similar, and that all aberrant nodules show an impaired bacteroid developmental progression from stage II to III. This suggests that the *MtENOD40* genes do not act redundantly in bacteroid development and, in contrast to their involvement in nodule initiation, neither acts synergistically. This shows that both *MtENOD40* genes are essential for bacteroid development.

It is likely that in the aberrant nodules, bacteroids are unable to fix nitrogen. In the nodules that do not show an impaired bacteroid development, it is expected that bacteroids are able to fix nitrogen. The present data are consistent with the observations in nodules formed on RNAi *LjENOD40-1* plants (Kumagai *et al*., 2006). Some of these *L. japonicus* nodules are also white and small, suggesting an impaired nodule development.

Here it is shown that *MtENOD40-1* and *MtENOD40-2* are both required for bacteroid development. This observation therefore offers an opportunity for unravelling the nature of the biological activity of *ENOD40*.

Acknowledgements

This work was supported by the Netherlands Organization for Scientific Research (WOTRO 86-160, XW) and the Erasmus Exchange Program (AI and CG).

References

Bergersen FJ. 1974. Formation and function of bacteroids. In: Quispel A, ed. *The biology of nitrogen fixation*. Amsterdam: North-Holland Publishing Company, 476–498.

Charon C, Sousa C, Crespi M, Kondorosi A. 1999. Alteration of *ENOD40* expression modifies *Medicago truncatula* root nodule development induced by *Sinorhizobium meliloti*. *The Plant Cell* **11,** 1953–1965.

Compaan B, Yang WC, Bisseling T, Franssen H. 2001. *ENOD40* expression in the pericycle precedes cortical cell division in *Rhizobium*–legume interaction and the highly conserved internal region of the gene does not encode a peptide. *Plant and Soil* **230,** 1–8.

Crespi MD, Jurkevitch E, Poiret M, d'Aubenton-Carafa Y, Petrovics G, Kondorosi E, Kondorosi A. 1994. *ENOD40*, a gene expressed during nodule organogenesis, codes for a non-translatable RNA involved in plant growth. *EMBO Journal* **13,** 5099–5112.

Fang YW, Hirsch AM. 1998. Studying early nodulin gene *ENOD40* expression and induction by nodulation factor and cytokinin in transgenic alfalfa. *Plant Physiology* **111,** 53–68.

Flemetakis E, Kavroulakis N, Quaedvlieg NEM, Spaink HP, Dimou M, Roussis A, Katinakis P. 2000. *Lotus japonicus* contains two distinct *ENOD40* genes that are expressed in symbiotic, nonsymbiotic, and embryonic tissues. *Molecular Plant–Microbe Interaction* **13,** 987–994.

Girard G, Roussis A, Gultyaev AP, Pleij CWA, Spaink HP. 2003. Structural motifs in the RNA encoded by the early nodulation gene *enod40* of soybean. *Nucleic Acids Research* **31,** 5003–5015.

Kouchi H, Hata S. 1993. Isolation and characterization of novel nodulin cDNAs representing genes expressed at early stages of soybean nodule development. *Molecular and General Genetics* **238,** 106–119.

Kouchi H, Takane K, So RB, Ladha JK, Reddy PM. 1999. Rice ENOD40: isolation and expression analysis in rice and transgenic soybean nodule development. *The Plant Journal* **18,** 121–129.

Kumagai H, Kinoshita E, Ridge R, Kouchi H. 2006. RNAi knock-down of ENOD40s leads to significant suppression of nodule formation in *Lotus japonicus*. *Plant Cell Physiology* **47,** 1102–1111.

Limpens E, Bisseling T. 2003. Signaling in symbiosis. *Current Opinion in Plant Biology* **6,** 343–350.

Limpens E, Mirabella R, Federova E, Franken C, Franssen H, Bisseling T, Geurts R. 2005. Formation of organelle-like N_2-fixing symbiosomes in legume root nodules is controlled by DMI2. *Proceedings of the National Academy of Sciences, USA* **102,** 10375–10380.

Limpens E, Ramos J, Franken C, Raz V, Compaan B, Franssen H, Bisseling T, Geurts R. 2004. RNA interference in *Agrobacterium rhizogenes* transformed roots of *Arabidopsis* and *Medicago truncatula*. *Journal of Experimental Botany* **55,** 983–992.

Nam Y-W, Penmetsa R, Endre G, Ubribe P, Kim D, Cook DR. 1999. Construction of a bacterial artificial chromosome library of *Medicago truncatula* and identification of clones containing ethylene-response genes. *Theoretical and Applied Genetics* **98,** 638–646.

Patriarca E, Tate R, Ferraioli S, Iaccarrino M. 2004. Organogenesis of legume root nodules. *International Review of Cytology* **234,** 201–263.

Ruttink T, Boot K, Kijne J, Bisseling T, Franssen H. 2006. *ENOD40* affects elongation growth in tobacco Bright Yellow-2 cells by alteration of ethylene biosynthesis kinetics. *Journal of Experimental Botany* **57,** 3271–3282.

Santi C, von Groll U, Ribeiro A, Chiurazzi M, Auguy F, Bogusz D, Franche C, Pawlowski K. 2003. Comparison of nodule induction in legume and actinorhizal symbiosis: the induction of actinorhizal nodules does not involve *ENOD40*. *Molecular Plant–Microbe Interaction* **16,** 808–816.

Scheres B, Van Engelen F, Van der Knap E, Van der Wiel C, Van Kammen A, Bisseling T. 1990. Sequential induction of nodulin gene expression in developing pea nodules. *The Plant Cell* **2,** 687–700.

Sonti RV, Chiurazzi M, Wong D, Davies CS, Harlow GR, Mount DW, Signer E. 1995. Arabidopsis mutants deficient in T-DNA integration. *Proceedings of the National Academy of Sciences, USA* **92,** 11786–11790.

Sousa C, Johansson C, Charon C, Manyani H, Sautter C, Kondorosi A, Crespi M. 2001. Translational and structural requirements of the early nodulin gene *enod40*, a short-open-reading frame-containing RNA for elicitation of a cell-specific growth response in the alfalfa root cortex. *Molecular and Cellular Biology* **21,** 354–366.

Spaink HP. 2000. Root nodulation and infection factors produced by rhizobial bacteria. *Annual Review of Microbiology* **54,** 257–288.

Stougaard J. 2001. Genetics and genomics of root symbiosis. *Current Opinion in Plant Biology* **4,** 328–335.

Timmers AC, Soupene E, Auriac MC, de Billy F, Vasse J, Boistard P, Truchet G. 2000. Saprophytic intracellular rhizobia in alfalfa nodules. *Molecular Plant–Microbe Interaction* **13,** 1204–1213.

Vance CP, Johnson LEB. 1983. Plant determined ineffective nodules in alfalfa (*Medicago sativa*): structural and biochemical comparisons. *Canadian Journal of Botany* **61,** 93–106.

Varkonyi-Gasic E, White DWR. 2002. The white clover *ENOD40* gene family. Expression patterns of two types of genes indicate a role in vascular function. *Plant Physiology* **129,** 1107–1118.

Vasse J, de Billy F, Camut S, Truchet G. 1990. Correlation between ultrastructural differentiation of bacteroids and nitrogen fixation in alfalfa nodules. *Journal of Bacteriology* **172,** 4295–4306.

Yang WC, Katinakis P, Hendriks P, Smolders A, de Vries F, Spee J, van Kammen A, Bisseling T, Franssen H. 1993. Characterization of *GmENOD40*, a gene showing novel patterns of cell-specific expression during soybean nodule development. *The Plant Journal* **3,** 573–585.